

# Fast Spatially Resolved Measurement of $R_2'$ and $R_2$ of each component of Cancellous Bone Marrow and Correlation of $R_2'$ with Trabecular Bone Volume Fraction (BVF)

C. E. Jones<sup>1</sup>, J. F. Magland<sup>1</sup>, A. Techawiboonwong<sup>1</sup>, F. W. Wehrli<sup>1</sup>

<sup>1</sup>Laboratory for Structural NMR Imaging, Department of Radiology, University of Pennsylvania Medical Center, Philadelphia, PA, United States

## Introduction

The difference in magnetic susceptibility between bone and bone marrow causes local perturbations of the magnetic field in the marrow spaces of cancellous bone. These, in turn, cause broadening of the marrow proton resonances of each spectral component from  $R_2/\pi$  to  $(R_2+R_2')/\pi$  (in Hz). Since  $R_2'$  increases with the density of trabeculae and their orientation relative to the polarizing field  $B_0$ <sup>1</sup> it has potential diagnostic value for diagnosing pathologies such as osteoporosis where trabecular architecture deviates from the architecture of healthy cancellous bone. Measurement of  $R_2^*$  can be ambiguous as  $R_2$  depends on marrow composition<sup>2</sup>. Further, analysis in the time domain is confounded by the multiple resonances that cause a modulation of the signal decays. In this work we acquire spectra by mapping the evolution of the signal before and after a phase-reversal RF pulse using a multiple-interleave GESFIDE<sup>3</sup> sequence. However, in distinction to earlier work, we generate spectra as the Fourier transform of the descending and, and separately, the ascending portion of the signal. From the resulting linewidths in the two sets of spectra,  $R_2'$  can be computed. As a means to examine the effectiveness of the technique, the trabecular bone volume fraction (BVF) was measured from high-resolution anatomic images acquired with the FLASE<sup>4</sup> sequence, and correlated with  $R_2'$  measurements.

## Methods

Both spectroscopic and high-resolution anatomic images were acquired with a custom-built dual phased-array coil, as sagittal slices of human radius and tibia specimens. Spectroscopic images were acquired with an interleaved GESFIDE<sup>3</sup> sequence, with the parameters: FOV =  $72 \times 54$  mm<sup>2</sup>, matrix =  $64 \times 48$ , slice thickness = 4 mm, pre-refocusing ETL = 16, post-refocusing ETL = 16, echo spacing = 6 ms, number of interleaves = 6, TR = 1 s. Echo time of the initial gradient echo was 4 ms and the echo time of the final gradient echo (which coincided with the spin echo) was 200 ms. The effective inter-echo time was 1 ms, resulting in a spectroscopic bandwidth of 1 kHz. Final voxel size after averaging  $3 \times 3$  pixels was  $3.375 \times 3.375 \times 4$  mm<sup>3</sup>. High-resolution anatomic images were acquired with a fast large-angle spin echo (FLASE)<sup>4</sup> sequence (matrix =  $512 \times 384 \times 32$  slices of 0.4 mm thickness, and  $137 \times 137$   $\mu\text{m}^2$  in-plane pixel size, TR = 110 ms, acquisition time = 16 min). The center of the FLASE slab was chosen coplanar with the center of the GESFIDE slice. Only the 10 FLASE slices located within the volume of the GESFIDE slice were included in BVF calculations.

Data were processed in IDL (Research Systems Inc, Boulder, CO). On a pixel by pixel basis, the pre- and post-refocusing time domain data were separated and Fourier transformed (FT), the post-180° data being reversed and complex-conjugated prior to transformation. When the irreversible portion of the transverse relaxation rate ( $R_2$ ) is less than the reversible portion (evolving as  $R_2'$ ) (a requirement verified experimentally for the dominant bone marrow component (Fig. 1)), the FT of post-refocusing pulse signal provides a spectrum of the bone marrow component whose linewidths are equal to  $R_2'/\pi = (R_2 - R_2')/\pi$ . For each voxel of interest (VOI)  $R_2'$  and  $R_2^*$  were calculated from spectra corresponding to the pre- and post-refocusing signals, respectively. The reversible transverse relaxation rate was then calculated as  $R_2' = \frac{1}{2} (R_2^* - R_2)$ .

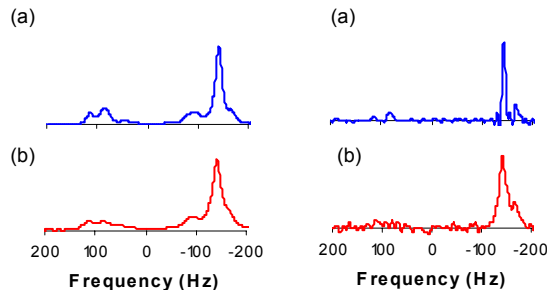


**Fig. 1**  $R_2^* = R_2 + R_2'$  spectra obtained from FT of FID, from voxel corresponding to blue (a) and red (b) ROIs indicated in Fig. 3.

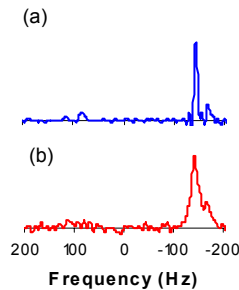


**Fig. 2**  $R_2' (= R_2^* - R_2)$  spectra obtained by FT of post-refocusing time domain data (see Methods), from voxels corresponding to blue (a) and red (b) ROIs indicated in Fig. 3.

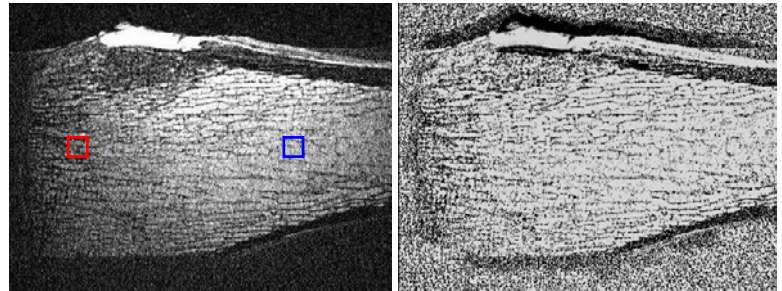


**Fig. 3** 3D high resolution sagittal image of a human tibia specimen, the red and blue ROIs correspond to the spectra shown in Figs. 1,2 (a); BVF map of the same slice (b).

## Results and Discussion

The spectra shown in Figs. 1 and 2 correspond to the VOI indicated in Fig. 3 (red and blue squares). Clearly, the  $R_2^*$  spectrum corresponding to the blue ROI located in the metaphysis (Fig. 1a) is narrower than the spectrum corresponding to the red ROI in the distal epiphysis (Fig. 1b), reflecting less dense trabecular architecture at this location<sup>5</sup>. The  $R_2'$  spectra (Fig. 2) are noticeably narrower than their  $R_2^*$  counterparts, consistent with the linewidth of the former being proportional to  $R_2 - R_2'$ , while the linewidth of the latter is proportional to  $R_2 + R_2'$ . Notice also the absence of components in the  $R_2'$  spectra (Fig. 2) that are present in the  $R_2^*$  spectra (Fig. 1), a consequence of their higher irreversible transverse relaxation rate. Fig. 4 displays a correlation between  $R_2'$  and BVF the human tibia bone showing the expected strong relationship between line broadening and trabecular density.

## Conclusion

Cancellous bone marrow  $R_2'$  can be directly measured from GESFIDE spectra acquired in a 5 minute acquisition time under *in vivo* conditions. Spectroscopic  $R_2'$  mapping of cancellous bone may provide a time efficient alternative to high-resolution imaging for assessment of bone quality.

**References:** (1) Yablonskiy D, *MRM* 1997;214-221 (2) Ma J and Wehrli FW. *JMR B* 1996;111:161. (3) Ma J et al., *MRM B* 1996;61:69. (4) Ma J et al., *MRM* 1996;903-10. (5) Majumdar M & Genant H, *JMRI* 1992: 209-219.

**Acknowledgement:** NIH grants ROI HL68908, ROI DJ063579

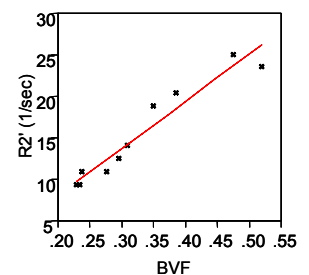


**Fig. 4**  $R_2'$  versus BVF for a human tibia specimen ( $r^2=0.93$ ,  $p=0.0001$ ). Symbols represent values from 10 individual regions.